http://dx.doi.org/10.1128/JVI.03014-13

Smyth, R.P., Schlub, T.E., Grimm, A.J., Waugh, C., Ellenberg, P., Chopra, A., Mallal, S., Cromer, D., Mak, J., Davenport, M.P. and Hahn, B.H. (2014) Identifying Recombination Hot Spots in the HIV-1 Genome. Journal of Virology, 88 (5). pp. 2891-2902.

JVI Accepts, published online ahead of print on 26 December 2013
J. Virol. doi:10.1128/JVI.03014-13

Identifying recombination hotspots in the HIV-1 genome.

Running title: HIV-1 recombination hotspots

RP Smyth[1,2,3,*], TE Schlub[4,*], AJ Grimm[5], C Waugh[7,8], Paula Ellenberg[1], A Chopra[6], S Mallal[6], D Cromer[5], J Mak[7,8#], MP Davenport[5#].

[1] Centre for Virology, Burnet Institute, Melbourne, Victoria, Australia
[2] Department of Biochemistry and Molecular Biology, Monash University, Clayton, Victoria, Australia
[3] Architecture et Réactivité de l'ARN, Université de Strasbourg, CNRS, IBMC, 15 rue René Descartes, 67084 Strasbourg, France
[4] School of Public Health, Sydney University, Sydney, New South Wales, Australia
[5] Centre for Vascular Research, University of New South Wales, Sydney, New South Wales, Australia
[6] Institute for Immunology and infectious diseases (IIID), Murdoch University, Perth, 6150, Australia
[7] School of Medicine, Faculty of Health, Deakin University, Geelong, Victoria, Australia
[8] Commonwealth Scientific and Industrial Research Organisation, Australian Animal Health Laboratory, Geelong, Australia.
*** These authors contributed equally to the work**
# Corresponding authors: johnson.mak@deakin.edu.au (JM), M.Davenport@unsw.edu.au (MD)

Abstract

HIV-1 infection is characterised by the rapid generation of genetic diversity that facilitates viral escape from immune selection and antiretroviral therapy. Despite recombination's crucial role in viral diversity and evolution, little is known about the genomic factors that influence recombination between highly similar genomes. In this study, we use a minimally modified full length HIV-1 genome and high throughput sequence analysis to study recombination in *gag* and *pol* in T cells. We find that recombination is favoured at a number of recombination hotspots, where recombination occurs six times more frequently than at corresponding coldspots. Interestingly, these hotspots occur near important features of the HIV-1 genome, but do not occur at sites immediately around protease inhibitor or reverse transcriptase inhibitor drug resistance mutations. We show that the recombination hot and cold spots are consistent across five blood donors and are independent of co-receptor mediated entry. Finally, we check common experimental confounders and find that these are not driving the location of recombination hotspots. This is the first study to identify the location of recombination hotspots, between two similar viral genomes with great statistical power and under conditions that closely reflect natural recombination events amongst HIV-1 quasispecies.

Statement of importance

The ability of HIV-1 to evade the immune system and antiretroviral therapy depends on genetic diversity within the viral quasispecies. Retroviral recombination is an important mechanism that helps to generate and maintain this genetic diversity, but little is known about how recombination rates vary within the HIV-1 genome. We measured recombination rates in *gag* and *pol* and identify recombination hot and cold spots demonstrating that recombination is not random, but depends on the underlying gene sequence. The strength and location of these recombination hot and cold spots can be used to improve models of viral dynamics and evolution, which will be useful for the design of robust antiretroviral therapies.

Introduction

The high level of genetic diversity is one of the main contributors to immune system and drug treatment failure during human immunodeficiency virus type 1 (HIV-1) infection. This diversity is primarily generated by the error prone reverse transcriptase during DNA synthesis, a process that results in approximately one mutation every three-replication cycles (1-4). Moreover, each HIV-1 virion contains two copies of the RNA genome, allowing the reverse transcriptase to switch between the two co-packaged RNA genomes. This process of recombination also influences HIV-1's sequence diversity by generating a progeny that is a genetic mix of the two parental strains (5). Recombination occurs much more frequently than mutation and is a powerful force that influences the evolution of the HIV-1 genome (for review see reference (4)). Investigations into locations of inter/intra subtype recombination indicate that sequence identity is sufficient to explain most breakpoint locations (6-9). This is unsurprising as sequence similarity between genomic partners is a strict requirement for efficient recombination (7, 10-12). Given that the vast majority of HIV-1 infections are not the result of co-infections with multiple divergent viral strains, but are initiated from a *single* virion, a model system that measures recombination between genetically similar genomes rather than inter/intra subtypes will better approximate the quasispecies *in vivo* (13-15). However, little is known about recombination likely to be found within the viral quasispecies of an infected individual because it is difficult to detect recombination between genetically similar genomes. Understanding recombination is a critical piece in the puzzle of HIV-1's evolutionary history and may help with the development of future treatments or with vaccine design.

Measuring recombination involves analysing the progeny of heterozygous virions (virions containing two genetically different genomes) to determine where recombination breakpoints exist, and at what frequency they are generated. Studies to date have measured recombination rates in a number of elegant ways. The use of retroviral reporter systems, where correctly positioned recombination will recreate a functional 'foreign' gene insert conferring antibiotic resistance or fluorescence (16-18) allows for the rapid screening of recombinants, but does not allow the measurement of recombination on the natural HIV-1 sequence. A more direct method of detecting recombination is through the sequencing of reverse transcription products derived from an authentic HIV-1 replication cycle. Importantly, recombination can only be observed when it leads to the generation of chimeric molecules. That is, template switching between identical genomes, or an even number of template switches between two genetic loci will lead to no genetic changes and will go unobserved. Thus to detect recombination on the native HIV-1 genome, genetically different strains must be utilized. Previous studies have leveraged sequence differences between highly divergent but naturally occurring subtypes to measure intra or inter-subtype recombination (19-22). However, as the overall sequence similarity between RNA templates is a major driving force governing recombination (6, 7, 10, 12), and the majority of infected individuals harbour viral populations that are known to be genetically similar (14, 23), measurements of recombination between genetically divergent strains will only reflect the special case of inter/intra subtype recombination but will not reflect recombination amongst the genetically similar HIV-1 genomes found in most viral quasispecies.

To address these issues, we developed a minimally codon modified HIV-1 genome and showed that this could be used to directly measure recombination under conditions where sequence similarity between RNA templates remains high (24). Using Sanger sequencing of single round reverse transcription products in the absence of selection, we showed that recombination does not occur randomly. This is in agreement with studies showing recombination rates depend on a complex set of factors, such as the availability of nucleotide substrates (25-27), the RNA template itself (7, 12, 28), overall sequence similarity (6, 7, 10, 12) and local sequence context of recombining sequences (28-30). Using both *in vitro* assays and single cycle HIV-1 vectors, recombination hotspots have been identified in the untranslated regions (UTRs) (30-32), in *gag* (29, 33) and in *env (28, 34)*. However, only limited information on recombination is available within other regions of the HIV-1 genome (33). We and others have attempted to use direct sequencing to locate recombination hotspots within the HIV-1 genome (24, 33, 35), but the large amount of sequencing data required made it impossible to draw firm conclusions with strong statistical support.

In this study, we made use of next generation sequencing to perform a comprehensive analysis of HIV-1 recombination using the marker method, with two marker configurations in *gag* and *pol* that allows recombination to be measured over 13 and 26 regions, respectively. This configuration is uniquely high resolution, with regions (separated by adjacent marker points) ranging from 21-159 nucleotides in length. Additionally, the system has broad coverage within *gag* and *pol*. We develop a statistical approach for comparing recombination rates and find that the recombination is not constant along the genome, but varies with nucleotide position. This variation is statistically significant, with some regions showing a six-fold difference in recombination rate. We identify 7 hotspots and 3 cold spots in *gag;* and 5 hotspots and 7 cold spots in *pol*. Hotspots appear in *gag* at the beginning of matrix, the matrix/capsid junction and the capsid/p2 junction and in *pol* at the protease-p51 junction. We found no hotspots around regions that have been implicated with protease inhibitor and reverse transcriptase inhibitor drug resistance mutations. We also analyse recombination rates using a virus with a completely different set of engineered marker points, and find that differences in recombination rate are not simply due to our silent marker manipulation of the viral sequence. Our results show that the viral gene region is a strong independent predictor of recombination rate.

Materials and Methods

Molecular Clones

pDRNLMK$_{low}$ (Genbank KC771033) and pDRNLMK$_{high}$ (Genbank KC771034) are minimally modified plasmids based on the prototypic HIV-1 strain pDRNL43. pDRNL43 is itself a derivative of pNL43, which originates from Ron Desrosiers (New England Primate Research Center) and is modified to remove 1.5Kb of cellular DNA flanking the HIV-1 genome in the pNL43 construct (36). The modified plasmids are altered in *gag* to include 17 and 15 marker points, and in *pol* to include 16 and 34 marker points for pDRNLMK$_{\text{low}}$ and pDRNLMK$_{\text{high,}}$ respectively. Marker points consist of, where possible, two single base pair changes in adjacent codons. This strategy allows us to distinguish easily between mutations introduced during the experimental procedure and real recombination. Furthermore, these marker points do not change any viral protein sequence or known RNA sequence elements, such a splice sites, and were rationally designed to minimize structural changes to the HIV-1 genome. Sequences were synthesised commercially (Genscript) and cloned into the ApaI and SpeI (*gag*) and XbaI and NotI (*pol*) sites of pDRNL43. pDRNLMK$_{\text{low}}$ and pDRNLMK$_{\text{high}}$ were converted from the X4 tropic phenotype to the R5 phenotype, to generate pDRNLAD8MK$_{\text{low}}$ and pDRNLAD8MK$_{\text{high}}$ by exchanging the Env gene from the pDRNLAD8 using the EcoRI and BamHI restriction sites. These modifications were well tolerated as the protein processing profile and the abilities to establish infection via reverse transcription were not affected, enabling us to accurately quantify the recombination processes during primary cell infection.

Recombination assay

We produced pools of homozygous virus (virus containing identical genomes) by transfecting wild type and marker virus plasmids separately, and produced heterozygous virus (virus containing two different genomes) by co-transfection of the wild type and marker plasmids. Viral particles from clarified transfection supernatants were further purified by sequential filtration through 0.8 µm and 0.45 µm sterile syringe filters (Sartorius). Purified virus was then concentrated by ultracentrifugation through a 20% sucrose cushion using an L-90 ultracentrifuge (Beckman Coulter) at 100,000 × g for 1 h at 4°C. Pellets were resuspended in media and the virus quantified by enzyme-linked immunosorbant assay (ELISA) (Vironostika). Concentrated virus stocks were supplemented with 2 mM MgCl2 and treated with 90 units/mL of Benzonase (Sigma) for 15 min at 37°C before infection to remove any contaminating plasmid DNA. Peripheral blood mononuclear cells (PBMCs) were isolated from buffy coats of HIV-1 seronegative blood donors (supplied by the Red Cross Blood Bank Service, Melbourne) by density gradient centrifugation over Ficoll-Plaque Plus (Amersham Biosciences). The identities of the blood donors from Red Cross are anonymous. Peripheral blood lymphocytes (PBLs) were purified from PBMCs and stimulated in media (2 × 10^6 cells/ml) supplemented with 10 µg/ml phytohemagglutinin (PHA) (Murex Diagnostics) and 10 units/ml human interleukin-2 (IL-2) (Roche Applied Science) for 2 days in Teflon-coated jars. After 2 days, PBLs were resuspended in fresh media containing 10 units/ml human interleukin-2 (IL-2) (Roche Applied Science) and incubated for a further 2 days before infection. Stimulated PBLs were infected with equal amounts of either homozygous or heterozygous virus, as determined by a HIV-1 antigen (p24 CA) micro ELISA assay. Heat inactivated (2 hr at 56°C) control infections were carried out to confirm efficient removal of plasmid DNA for each sample. 6 hr post-infection 10 µg/mL T-20 (NIH AIDS Reagent Program) was added to the cells to prevent second round replication. At 24 hr post PBL infection, cells were lysed and full-length reverse transcriptase products were quantified. Reverse transcription products were amplified using 10 sets of primers, generating 10 overlapping PCR amplicons (see primers). The following 2-step cycling conditions were chosen to minimize PCR induced recombination, as previously described (37): initial copy number 2,500, denaturation 98°C for 30 sec, followed by 72°C for 2 min for 29 cycles. PCR products for sequencing were created by pooling at least 4 independent PCR reactions per condition. Unique 6 nucleotide identifiers (barcodes) were attached using a modified parallel tagged sequencing protocol to allow multiplexing on the same sequencing run (38). Emulsion PCR and sequencing were performed at the Institute for Immunology and Infectious Diseases (IIID), Perth, according to standard GS FLX titanium procedures. In order to avoid re-sampling, we generated our sequencing libraries in such a way as to ensure that it contained PCR products generated from over 10,000,000 original DNA molecules per plate of 454 sequencing run, whereas a single 454 sequencing run has sequencing capacity of ~1 million reads. We note that in any event, resampling per se would not lead to an increase in recombination rates.

Primers

Overlapping PCR amplicons for sequencing were generated using 10 sets of primers: G1(2945)Fw GAGATGGGTGCGAGAGCGTC and G1(3314)Rv TGTGTCAGCTGCTGCTTGCTG; G2(3236)Fw ACCAAGGAAGCCTTAGATAAGATAGAGGAAGAG and G2(3679)Rv

TGAAGGGTACTAGTAGTTCCTGCTATGTCACTTC; G3(3584)Fw GATAGATTGCATCCAGTGCATGCAG and G3(3955)Rv GCTTTTAAAATAGTCTTACAATCTGGGTTCGC; G4(3793)Fw TCTGGACATAAGACAAGGACCAAAGG and G4(4195)Rv ACATTTCCAACAGCCCTTTTTCCTAG; P1(4433)Fw GCGACCCCTCGTCACAATAAAGATAG and P1(4884)Rv GAGTATTGTATGGATTTTCAGGCCCAAT; P2(4695)Fw CACTTTAAATTTTCCCATTAGTCCTATTGAGACTG and P2(5110)Rv ACTAGGTATGGTAAATGCAGTATACTTCCTGAAG; P3(4951)Fw AAGAGAACTCAAGATTTCTGGGAAGTTCA and P3(5325)Rv CTCAGTTCCTCTATTTTTGTTCTATGCTGC; P4(5233)Fw CCAGACATAGTCATCTATCAATACATGGATGA and P4(5618)Rv CCAGTTCTAGCTCTGCTTCTTCTGTTAGTG; P5(5503)Fw TGGGCAAGTCAGATTTATGCAGG and P5(5934)Rv GTGGCTTGCCAATACTCTGTCCAC; P6(5774)Fw GAATGAAGGGTGCCCACACTAATG and P6(6166)Rv GCAAAGCTAGATGAATTGCTTGTAACTCAG.

Data Processing

In order to align, process and categorise the very large volume of sequencing data (>1 million sequences) that result from next generation sequencing, we used *EMBOSS needle* ***(39)*** and custom software written in BioRuby ***(39)***. After alignment to the genome, each sequence read was processed to identify regions that cover two markers points. Each region was then classified as recombination observed (if marker endpoints switched between marker type and wild type virus) or recombination not observed (if marker endpoints were identical). It is important to note that our marker points were designed so that all marker point contained at least two mutations in usually adjacent codons. Consequently, it is very unlikely that mutations introduced by the experimental setup, infection process or sequencing will artificially signal recombination. This is confirmed by the low rates of recombination in our controls. However, several marker points did exhibit poor sequence quality and alignment (regions P_H1, P_H2, P_H3, P_H4, P_H5, P_L1, P_L2 and P_L3, likely due to the presence of indels (either naturally or introduced by the marker point). As 454 sequencing has known issues with homopolymer sequences (40), and the sequence quality around these markers is vital for our analysis, the marker points showing poor sequence alignment (shown in black in Figure

4) are excluded from the analysis. These excluded markers and bordering regions represented a small fraction (~10%) of the pre-cleaned data.

Recombination rates

Recombination rates and confidence intervals were calculated in the statistical package R (41) using the linear model function "lm" on the optimal recombination rate, *r*, over all genome regions. For each interval, the recombination rate is calculated as

$$r = \frac{-\ln{(1-2a)}}{2L} \tag{1}$$

where *L* is the nucleotide length of the genome region and *a* is the proportion of heterozygous sequences that observe a recombination for that region. This equation compensates for the probability of multiple (and therefore unobserved) recombination events between marker points (24). The number of heterozygous sequences is expected to be 50%, however this is directly estimated from the homozygous sequence frequency of each virus type using the method described in Schlub et. al. (24). The calculated recombination rate will represent an average recombination rate for each interval as the precise nucleotide position of the recombination event cannot be determined within the interval where parental sequences are identical.

Comparing recombination rates

We use two distinct marker configurations, where codon modifications occur on different nucleotides, to test if the choice of marker nucleotide position influences recombination rate fluctuations. To compare the results from the two configurations, we use marker system 1 to predict the recombination rate in marker configuration 2, and correlate this prediction with the experimental data for marker configuration 2. For each region in marker configuration 2, the prediction is calculated as the weighted average of recombination rates in overlapping regions from marker configuration 1, where the weighting is the proportion overlap (Figure 4B).

Correlations between datasets are performed in the statistical package R (41), using the 'cor.test' function. Correlations are Pearson correlations unless otherwise stated. When correlating between marker configuration 1 and 2, adjacent regions in the marker configuration 1 prediction of marker configuration 2 will not be independent if a region from configuration 1 overlaps with two regions in configuration 2. To check whether this influences the correlation results presented, we define the dependence between two predictions that share an overlapping marker configuration 1 region to be the minimum weighting (percentage overlap) for those overlapping regions. Predictions with a dependence value over 10% are systematically removed to keep the maximal amount of data. The correlation coefficients and corresponding p-values resulting from this removal do not change substantially from those presented in the figures, and no significance levels or conclusions would be changed. Additionally using the non-parametric Spearman Rank correlation instead of the Pearson correlation does not change the significance of correlation co-efficient nor any of the conclusions.

Controls for experimentally-associated recombination

Our primary focus is on the viral recombination induced during reverse transcription of the HIV-1 genome *in vitro*. However, recombination can also be experimentally induced at different stages of the procedure, such as during transfection of cell with plasmid, during PCR amplification, or during sequencing (37, 42-44). To ensure that the recombination rates presented are representative of the recombination rates experienced during a single cycle of HIV-1 replication, we comprehensively measured potential sources of artificial recombination.

To measure any background recombination that might arise as a result of plasmid transfection and PCR amplification, we performed a number of controls. First, RNA was extracted from heterozygous virus using phenol chloroform based TRI reagent (Sigma Aldrich) according to the manufacturer's recommendations and reverse transcribed into cDNA using SuperScript^{TM}III (SSIII) (Invitrogen Life Technologies) and gene specific primer GAG4(4195)R: 5'ACATTTCCAACAGCCCTTTTTCCTAG 3'. This measured the transfection recombination rate to be approximately 5x10^{-6} REPN (recombination events per nucleotide per round of infection), which corresponds to 0.25% of the total recombination rate reported in this study. To control for potential recombination during *in vitro* cell -free reverse transcription, we also performed the same reverse transcription and processing on a mix of homozygous WT virus and homozygous MK virus (mixed in equal quantities (based on p24 values) prior to RNA extraction, and were reverse transcribed in parallel with RNA extracted from heterozygous virus). We measure this rate to be $3x10^{-6}$ REPN (representing over half of the recombination occurring during our transfection control). Given that the recombination induced by SSIII is not present in our regular assay, this indicates that recombination occurring during transfection is even lower than our measured $5x10^{-6}$ REPN rate. Reverse transcription was performed in the presence and absence of SSIII, the latter condition providing a control for any plasmid contamination carried over from transfection. Real time PCR was used to estimate viral cDNA copy number against a standard curve based on plasmid pDRNL(AD8) using primers GAG1(2945)F: 5' GAGATGGGTGCGAGAGCGTC 3' and GAG1 (3314)R: 5' TGTGTCAGCTGCTGCTTGCTG 3'. Again, template viral cDNA were amplified using optimized PCR conditions outlined in the recombination assay section above.

To assess background recombination introduced by PCR, we amplified a 1:1 mixture of WT and MK plasmid and sequenced the resulting DNA (PCR control plasmid). As a more stringent PCR control, we infected cells with an equal mixture of homozygous wild type and homozygous marker virus and subsequently PCR amplified and sequenced the resultant cDNA (PCR control cDNA). As each infection is the product of a homozygous virion, any intra-virion recombination will be effectively 'silent' (since both strands are identical). Thus any recombination observed between WT and MK virus must have occurred due to chimera formation during PCR amplification (or less likely due to recombination occurring between virions in the infected cell). We calculate the average cumulative background rate of PCR induced recombination to be $2.9x10^{-4}$ REPN, well below that of the recombination rate in the experimental sample. Three regions (G_H1, P_H23 and P_H25) did exhibit a higher risk of recombination in some (but not all) controls. As a precaution, these were removed from all data analysis (Figure 4). After removal, the average induced recombination rate was 2.2x10^{-4} REPN.

Generalized linear models

Generalized linear models (GLMs) were performed in the statistical package R (41), using the ‘glm’ function with a binomial error distribution. For each region the relationship between the estimated parameter (recombination rate) and experimental data (number of observed recombinations) depends on region nucleotide length and the proportion of heterozygous sequences (equation 1). To compensate for these factors, and ensure the binomial error distribution a custom link function identical to equation 1 was used. The factors viral phenotype, blood sample donor and interval region were tested with a process of forward addition. Statistical significance of the covariates was tested using a chi-squared test during an analysis of deviance.

Results

Experimental system

We developed a system that can measure recombination between highly similar genomes by rationally designing codon modifications into the full length HIV-1 genome. This system contains no foreign gene inserts that could alter the folding of the RNA genome, and we avoided RNA sequences that were known to fold into functional RNA structures, such as splice or frameshifting sites. We further minimized structural changes to the RNA genome by only using silent adenine-to-guanine or cytosine-to-thymine (uracil) substitutions. That is, whilst all genetic changes have the potential to alter RNA structure, adenine and guanine both form Watson-Crick base pairs with the RNA base uracil. Similarly, cytosine and thymine (uracil) both form Watson-Crick base pairs with the guanine. We reasoned that these substitutions are likely to have the least impact on global RNA structure, as they do not disrupt pre-existing base pairing. Finally, wherever possible, substitutions were only made if they occurred naturally in the HIV sequence compendium (45). These codon modifications do not change the ability to establish infection and the synthesis of viral cDNA via reverse transcription. These modifications create 39 genome regions ranging from 21nt to 159nt in length over which recombination can be studied. We produced pools of homozygous virus (virus containing identical genomes) by transfecting wild type and marker virus plasmids separately, and produced a mixture of homozygous and heterozygous virus (virus containing two different genomes) by co-transfection of the wild type and marker plasmids. We performed a single round infection in peripheral blood mononuclear cells (PBMCs) with pools of heterozygous and homozygous virions, after which recombination can be detected with high throughput sequencing of cDNA. The recombination rate between marker points was calculated with equations that (1) estimate the ratio of heterozygous to homozygous infections (2) compensate for the nucleotide length over which recombination is measured and (3) compensate for the probability of multiple (unobserved) recombination events between marker points (24) (see materials and methods).

Recombination rate fluctuates within gag and pol.

We first measured the recombination rate across our two regions of interest in *gag* and *pol*. We sequenced approximately 86,000 genome regions pooled from 5 donors and measured an average recombination rate of 2.0x10^{-3} recombination events per nucleotide per round of infection (REPN), corresponding to approximately 19-20 recombination events per genome (95% C.I. 1.8x10^{-3} to 2.2x10^{-3} REPN). When we segregated our data into the two regions, *gag* and *pol*, we found weak evidence for a different recombination rate, with an average recombination rate of 2.3x10^{-3} and 1.8x10^{-3} REPN, respectively (p=0.07, t-test on interval recombination rates). An advantage of our high-resolution marker system is the ability to investigate if recombination levels change with nucleotide position. Interestingly, we found a large level of fluctuation in recombination rate in different segments of the genome, where individual genome region's rates vary from 0.51x10^{-3} REPN to 3.4x10^{-3} REPN – a greater than 6-fold difference (Figure 1). This indicates that the recombination rate is not constant along the HIV-1 genome and that recombination hot and cold spots may exist.

To investigate this further, we sought to determine if the locations of putative recombination hotspots were consistent across two viral phenotypes that enter different subpopulations of T-lymphocytes via distinct co-receptors (CCR5 and CXCX4), and between unrelated blood donors. We found a significant and high correlation for the recombination rates in identical intervals when we compared between the R5 and X4 viral phenotype ($r = 0.69$, $p < 0.0001$, Figure 2A-B), and between blood donors (Figure 2C, Table 1). This provides strong evidence that the locations of putative recombination hotspots are similar between these groups, and also constant across multiple independent infection experiments, indicating a systematic change in recombination rate along the genome.

The recombination rates presented above theoretically include the cumulative effect of experimentally induced recombination during DNA transfection and subsequent PCR (46). To demonstrate that these experimentally induced rates are not the source of recombination hotspots, we independently measured the experimentally induced recombination rates (see Materials and Methods). We addressed whether transfection induced recombination could influence our recombination rates by directly measuring recombination rates on RNA extracted from heterozygous virions produced from cells co-transfected with WT and MK plasmids. We used SuperScript III (RNaseH-, recombination defective) to reverse transcribe RNA before subjecting it to PCR and sequencing using the same conditions as the experimental samples. This experiment measured the accumulation of recombination due to transfection, *in vitro* SuperScript III reverse transcription and PCR. This rate was calculated to be $5x10^{-6}$ REPN. For completeness, we also included two controls to dissect the contribution of PCR induced recombination and a further control to measure the contribution of SuperScript III recombination (see Materials and Methods). Although we did see some variation in the level of experimental recombination between experimental replicates, under all cases, we found that overall recombination rates were too low to introduce significant bias, in agreement with our previous results (24). We also measured the rate of recombination for each interval and found that the infrequent experimental recombination was not localised to hotspots but evenly spread over *gag* and *pol* (data not shown) Three regions (G_H1, P_H23 and P_H25) did exhibit a higher risk of recombination in some (but not all) controls. As a precaution, these were removed from the analysis for this paper (see materials and methods). To further check that these low levels of recombination are not driving the recombination hotspots we correlate the recombination rate between intervals in our experimental and biological sample. We found that the recombination rates following infection do not significantly correlate with the experimentally induced recombination rate (PCR cDNA recombination rate $r = 0.02$, $p = 0.93$; transfection recombination rate: $r = 0.03$, $p = 0.93$) (data not shown). Therefore the rates presented in this study are not biased by the experimental method, and provide an accurate view of HIV-1 recombination hotspots within the genome regions defined by our marker points.

Recombination rate hotspots are not a product of experimental marker design

The HIV-1 genome used in this study includes a number of introduced silent codon modifications to act as markers for recombination. These modifications were designed so that they did not alter any viral proteins or known RNA elements. However, as nucleotide sequence can influence recombination frequencies (47), we sought to investigate whether the choice of codon modifications was driving the variation in recombination rate observed in Figure 1. To test this, we created an additional viral phenotype MK_{low} with more broadly spaced marker points at different nucleotide positions within *gag* and *pol* (original phenotype: MK_{high})(Figure 4A, schematic of two marker systems). As with MK_{high}, these modifications do not change the viral protein sequence or the *in vitro* infectivity of the virus (data not shown). If the putative recombination hotpots measured in MK_{high} (Figure 1) are purely driven by sequence disruption due to codon modification, then the location of the hotspots in marker system MK_{low} will be different (as markers are at different nucleotide positions). Conversely, if the hotspot locations for MK_{high} and MK_{low} are similar, then this provides evidence that the variations in recombination rates are intrinsic to the viral genome and not a product of our codon modification.

The regions that measure the recombination rate in the two marker systems do not perfectly align (due to different marker codon nucleotide position, Figure 4) which makes it difficult to directly compare recombination rates at different sites between the two marker systems. To overcome this, the recombination rates from marker system MK_{high} were interpolated to predict the recombination rate using the new (more broadly spaced) marker system MK_{low} (Figure 4B, schematic of interpolation between marker systems, materials and methods). In this way, the recombination rates expected from the experimental rates in MK_{high} and the overlap between MK_{high} and MK_{low} can be compared with the experimentally observed rates for MK_{low} using a correlation analysis. Although this interpolation from high resolution to low does reduce the information available in the high resolution, and increase variability making a correlation harder to detect, it is necessary to directly compare the resolutions. We found that the recombination rate between marker sets is significantly correlated (r = 0.42, p = 0.03 for R5, r = 0.72, p < 0.001 for X4, Figure 3A-D) indicating that in general genomic regions with a high/low recombination rate in MK_{high} also have a high/low recombination rate in MK_{low}. Therefore recombination hotspot locations are consistent between the marker systems and these hotspots are not driven by the experimental codon modification.

Finally, recombination rate variation may be influenced by other experimental factors and sampling error (together called ‘random variation’ for simplicity). To estimate how much random variation exists for this study, we correlate two identical experiments with identical marker systems (both MK_{high}). If there were zero random variation, these two results should be identical and correlate perfectly. Therefore any deviation here provides a measure for the random variation in this study (Figure 3E-F). We found a high rate of correlation between experimental replicates (Figure 3F, r= 0.78, p < 0.001), further highlighting that putative recombination hotspots are intrinsic to the HIV-1 genome and not a product of other experimental factors.

Identifying the recombination hot and cold spots.

We have shown that our procedure reliably estimates local recombination rate changes in *gag* and *pol* and that these changes are consistent across viral phenotypes, blood donors, and codon marker systems. Thus, the identified changes of recombination rate across the viral sequences are intrinsic to the HIV-1 genome. However to accurately determine *hot* or *cold* spots with recombination rates significantly different to the average, a number of additional factors need to be considered. These include: the estimated number of sequences sampled for each interval; the variance introduced by unrelated blood donors; and the variance introduced by the target cell (controlled by the two viral phenotypes, CCR5 and CXCR4). Generalized linear models (GLMs) provide an analytic framework for investigating the relationship between recombination rate and genomic position whilst accounting for the factors listed above. Generalized linear models *generalize* a multiple regression analysis, allowing for the binomial distribution of our sequence recombination data, and the adjustment for interval nucleotide length when calculating recombination rates.

We used a process of forward addition to test and build the final GLM and to identify which covariates are significantly associated with recombination rate (Table 2). We find that recombination rate is significantly associated with viral phenotype (X4/R5, $p < 0.001$) and blood sample donor ($p < 0.001$) (chi-square test on analysis of deviance). We also find that the interval along the genome over which recombination is measured is also significantly associated with recombination rate ($p < 0.001$). The final model which include viral phenotype, blood sample donor, and interval, provides very strong evidence that the recombination rate is not constant over *gag* and *pol*, and that this result is consistent over viral phenotype and blood sample donor. This final GLM estimates the recombination rate parameter for each interval. By calculating the standard error for these parameter estimates, the intervals with a recombination rate significantly different to the average rate, that is recombination hot/cold spots, can be identified.

Over the 39 regions, we found 12 statistically significant recombination hotspots and 10 statistically significant recombination coldspots (Figure 5, Table 3). Interestingly, these hot and cold spots are unequally distributed in *gag* and *pol*, with *gag* containing seven of the twelve hotspots, yet only three of the ten coldspots. In *gag*, hotspots appear to cluster around gene junctions, at the beginning of matrix, the matrix/capsid junction and the capsid/p2 junction (Figure 5B). In *pol*, we find one hotspot at the protease-p51 junction (Figure 5B), but find no hotspots in genome regions containing mutations that have been implicated in drug resistance. Therefore, recombination is less likely to influence the generation of multiple drug resistant HIV-1 within these regions as compared to regions of the HIV-1 genome containing recombination hotspots for the generation of recombinant HIV-1.

Discussion

The high replication rate of HIV-1 combined with high rates of mutation and recombination lead to remarkable adaptability of the virus in the face of intense evolutionary pressure. Recombination is thought to make natural selection more efficient by breaking linkages between mutations (48-50). That is, recombination helps to maintain genetic diversity by breaking linkages between advantageous and deleterious mutations, whilst also facilitating the removal of deleterious mutations by bring them together in the same genome. Importantly, recombination can also pair advantageous mutations, which can facilitate the acquisition of multiple drug resistance leading to treatment failure (48-54). Recombination may also be an important mechanism by which the virus eventually escapes immune control (55-58). However, recombination also has the potential to inhibit adaptation and evolution depending on epistasis and genetic drift (51). Consequently, an improved understanding of recombination is important for understanding the evolutionary history of HIV-1 and may help to guide the design of robust antiretroviral therapies.

There have been many studies showing that even in the absence of selection recombination does not occur randomly on the HIV-1 genome, highlighting the presence of additional factors governing the recombination process (11, 19, 28-35, 59). However, many of these studies do not measure recombination rate in their natural genome context, or they measure recombination between highly divergent genomes that may not be most representative of the situation *in vivo*, where we expect recombination between closely related members of the viral quasi-species. Here, we present a system that allows the study of recombination between highly similar genomes that mimic the HIV-1 quasispecies within an HIV-1 infected patient. We delineate the process of retroviral recombination through infection of primary T lymphocytes with a minimally codon modified full-length virus. An advantage of this method is that we can target specific areas of the genome whilst controlling the length of interval and hence the accuracy of our study. We have previously used a similar system to analyse recombination rates in a small region of *gag* (37). In this case, we were unable to draw conclusions about the location of recombination hotspots primarily because this requires analysis of large numbers of sequences (19, 35, 37). In this study, we applied next generation sequencing to systematically measure at high-resolution recombination rates in *gag* and *pol*. These two genome regions were chosen because of their importance in the generation of drug resistant virus and immune escape mutations (60).

We have optimised this system and shown that it is not biased by confounding factors related to experimentally induced recombination and for the occurrence of multiple template switches over intervals of varying lengths (24, 37). Using two independent sets of marker modification, we show that putative recombination hotspots are not due to modifications introduced by our marker system. Indeed, there is a high correlation of recombination hotspots between our two systems. Notably, regardless of viral phenotype and blood donor, we demonstrate greater than 6-fold recombination rate changes across *gag* and *pol.* These changes are consistent regardless of viral phenotype (r = 0.68, p < 0.001) and blood donor (r = 0.44-0.71, p = <0.001 – 0.04). We identify 12 genome regions with significantly higher rates of recombination and 10 genome regions with significantly lower rates of recombination.

It is instructive to compare our recombination hotspots between closely related genomes with those identified in natural HIV-1 sequences. Surprisingly, the *gag* hot/cold spots identified in our study match closely with those identified by analysing patient sequences (6, 9, 61). This is surprising because regions of sequence similarity are presumed to drive inter-subtype recombination, and one would not expect to see the impact of local recombination hotspots after so many confounding factors such as selection for functional proteins, drug resistance or from the immune system (9, 62). One of the most comprehensive studies, by Simon-Loriere and colleagues analysed sequences retrieved from the Los Alamos National Laboratory HIV sequence database (http://hiv-web.langl.gov) provides evidence of recombination (9). Their study identified two hot spots and one cold spot in capsid of *gag*, corresponding to our regions G_H5-G_H8, G_H12-G_H13 and G_H9-G_H10, respectively. These regions also corresponded to hot and coldspot clusters in our analysis. The hot region spanning G_H5-G_H8 does include a sub-region with a strong and significant cold spot (G_H6; -0.73x10^{-3}, p<0.0001) that is not present in the Simon-Loriere study. However, this sub-region may have been missed in their data set as the segment G_H6 is only 21 bp in length, and they averaged their recombination breakpoints using a sliding window of 200 nt. It is interesting to note that these two hot regions span the Matrix-Capsid and Capsid-P2 junctions of Gag. Indeed, it has been proposed that the distribution of RNA structures along the HIV-1 genome has evolved to facilitate gene swapping in a way that maximises genetic diversity whilst minimizing the chance that the resulting progeny is impaired (9, 61). Our study does not directly address this issue as our marker points were designed to minimize structural changes to the genome. However, our data showing the position of hot and cold spots in the genome will help to inform future mechanistic studies into the factors that influence recombination.

Within *pol*, some of our hot spots do not match those found by analysing patient sequence databases. In our data set, we observe a hotspot near the beginning of p51 (P_H6; 0.74x10^{-5}; p<0.05) that is followed by a region of intermediate recombination ending with a strong recombination cold spot at P_H12 (-0.66x10^{-5}; P<0.0001). In the Simon-Loriere study, they identify a broad hot spot beginning at region P_H6 and peaking at P_H11. Thus, where their study finds one of their strongest hot spots, we find a region of intermediate recombination ending with one of our coldest spots at P_h12. As this region contains important resistance mutations, such as the thymidine analogue mutations (TAMS) (60), the detection of hotspots for recombination in the *in vivo* data could be evidence for selection. Similarly, we identify a cold spot (P_H31; $-0.75X10^{-5}$; $P<0.001$) that falls close to the p51-RNase H junction, which was labelled as a hotspot for recombination in the Simon-Loriere study. On the other hand, we identify hot spot P_H19 ($0.54x10^{-5}$; <0.05), which falls within an unstructured peptide loop of RT (63). Interestingly, this hot region P_H19-$_H21$ corresponds exactly to some of the most highly structured RNA in the HIV-1 genome, as measured by SHAPE chemistry (63). Indeed, RNA structures are proposed to favour recombination by causing reverse transcriptase to pause on the template (12, 27, 64-66), and mechanistic studies demonstrate that the presence of RNA structure is often a feature of recombination hotspots (34, 67). It has been previously reported that HIV-1 gene junctions are both enriched in RNA structure and thus more recombinogenic than other regions of the HIV-1 genome (61, 63) We anecdotally note that our recombination hot spots do seem to be enriched at gene junctions, with the exception of the RNase H junction. This suggests that local fluctuations in recombination rates could drive the evolution of the RNA genome on a global scale. Further investigation of these genomic locations is warranted as the molecular mechanisms that cause recombination hot and cold spots may shed further light on the higher-level organisation of the HIV-1 genome.

As recombination is thought to facilitate viral evolution by intermixing immune escape and drug resistance mutations within HIV-1 *gag* and *pol*, knowledge of how recombination rates vary within these particular (68) regions of the viral genome is of importance for designing antiviral strategies. From a therapeutic viewpoint, the shuffling of resistance mutations within *gag* and *pol* could impact the generation of multiple drug resistant virus (48-50). In general, the further apart genomic regions are, the less likely they will be linked together, and the easier it will be to shuffle mutations between these regions. For genomic regions that are close together, it should be easier to generate a RT double mutation where the resistance mutations are separated by a recombination hotspot. Our data suggests the major reverse transcriptase drug resistance mutations lie in a relatively stable region of the genome, theoretically 'reducing' the risk that they will be brought together by recombination. It is important to note, however, that an important prerequisite for recombination is the co-packaging of genetically distinct genomes into viral particles via efficient co-infection of cells. Early studies suggested that these conditions were likely to be fulfilled *in vivo*, with between 75-80% of infected spleen cells harbouring at least two or more proviruses, with most of these cells harbouring genetically distinct proviruses. (69). More recent studies on both CD4+ T cells and infected spleen cells contradict this view, and show that the majority of cells are only singly infected (68, 70). Nevertheless, there is ample evidence that at least some recombination does occur *in vivo*, and that it is functionally relevant to immune escape and the generation of multiple drug resistant HIV-1 (48-52, 54-58, 68). Furthermore, it is possible that the location of recombination hotspots may be more important under scenarios of low co-infection compared to scenarios where the conditions for recombination are rampant. It will be important to test this assertion by including the possibility of recombination hotspots in models of HIV-1 dynamics.

Altogether, our data provide unique insights into HIV-1 recombination occurring between highly similar genomes likely to be found in the majority of infected individuals. Our results demonstrate that recombination does not occur randomly, and we identify recombination hot-spots and cold-spots in *gag* and *pol*. Importantly, our recombination hot / cold spots match closely with those found by analysis of patient sequence databases, indicating that, for *gag* and *pol*, the recombinogenic properties of RNA genome itself, rather than sequence similarity is likely to be the main driver of recombinant genomes circulating in the human population. Further studies into this area may ultimately prove crucial in developing robust antiviral strategies against HIV-1.

Acknowledgements

The authors would like to thank Matteo Negroni for critical reading of the manuscript.

References

1. **Abram ME, Ferris AL, Shao W, Alvord WG, Hughes SH.** 2010. Nature, position, and frequency of mutations made in a single cycle of HIV-1 replication. J Virol **84:**9864-9878.
2. **Mansky LM, Temin HM.** 1995. Lower In Vivo Mutation Rate of Human Immunodeficiency Virus Type 1 than That Predicted from the Fidelity of Purified Reverse Transcriptase. J. Virol. **69:**5087-5094.
3. **Mansky LM.** 1996. Forward mutation rate of human immunodeficiency virus type 1 in a T lymphoid cell line. AIDS Res Hum Retroviruses **12:**307-314.
4. **Smyth RP, Davenport MP, Mak J.** 2012. The origin of genetic diversity in HIV-1. Virus Res.
5. **Hu WS, Temin HM.** 1990. Genetic consequences of packaging two RNA genomes in one retroviral particle: pseudodiploidy and high rate of genetic recombination. Proceedings of the National Academy of Sciences of the United States of America **87:**1556-1560.
6. **Archer J, Pinney JW, Fan J, Simon-Loriere E, Arts EJ, Negroni M, Robertson DL.** 2008. Identifying the important HIV-1 recombination breakpoints. PLoS Comput Biol **4:**e1000178.
7. **Baird HA, Galetto R, Gao Y, Simon-Loriere E, Abreha M, Archer J, Fan J, Robertson DL, Arts EJ, Negroni M.** 2006. Sequence determinants of breakpoint location during HIV-1 intersubtype recombination. Nucleic Acids Res **34:**5203-5216.
8. **Baird HA, Gao Y, Galetto R, Lalonde M, Anthony RM, Giacomoni V, Abreha M, Destefano JJ, Negroni M, Arts EJ.** 2006. Influence of sequence identity and unique breakpoints on the frequency of intersubtype HIV-1 recombination. Retrovirology **3:**91.
9. **Simon-Loriere E, Galetto R, Hamoudi M, Archer J, Lefeuvre P, Martin DP, Robertson DL, Negroni M.** 2009. Molecular mechanisms of recombination restriction in the envelope gene of the human immunodeficiency virus. PLoS Pathog **5:**e1000418.
10. **An W, Telesnitsky A.** 2002. Effects of varying sequence similarity on the frequency of repeat deletion during reverse transcription of a human immunodeficiency virus type 1 vector. J Virol **76:**7897-7902.
11. **Magiorkinis G, Paraskevis D, Vandamme AM, Magiorkinis E, Sypsa V, Hatzakis A.** 2003. In vivo characteristics of human immunodeficiency virus type 1 intersubtype recombination: determination of hot spots and correlation with sequence similarity. J Gen Virol **84:**2715-2722.
12. **Song M, Balakrishnan M, Chen Y, Roques BP, Bambara RA.** 2006. Stimulation of HIV-1 minus strand strong stop DNA transfer by genomic sequences 3' of the primer binding site. J Biol Chem **281:**24227-24235.
13. **Novitsky V, Wang R, Margolin L, Baca J, Rossenkhan R, Moyo S, van Widenfelt E, Essex M.** 2011. Transmission of single and multiple viral variants in primary HIV-1 subtype C infection. PLoS One **6:**e16714.
14. **Keele BF, Giorgi EE, Salazar-Gonzalez JF, Decker JM, Pham KT, Salazar MG, Sun C, Grayson T, Wang S, Li H, Wei X, Jiang C, Kirchherr JL, Gao F, Anderson JA, Ping LH, Swanstrom R, Tomaras GD, Blattner WA, Goepfert PA, Kilby JM, Saag MS, Delwart EL, Busch MP, Cohen MS, Montefiori DC, Haynes BF, Gaschen B, Athreya GS, Lee HY, Wood N, Seoighe C, Perelson AS, Bhattacharya T, Korber BT, Hahn BH, Shaw GM.** 2008. Identification and characterization of transmitted and early founder virus envelopes in primary HIV-1 infection. Proceedings of the National Academy of Sciences of the United States of America **105:**7552-7557.
15. **Abrahams MR, Anderson JA, Giorgi EE, Seoighe C, Mlisana K, Ping LH, Athreya GS, Treurnicht FK, Keele BF, Wood N, Salazar-Gonzalez JF, Bhattacharya T, Chu H, Hoffman I, Galvin S, Mapanje C, Kazembe P, Thebus R, Fiscus S, Hide W, Cohen MS, Karim SA, Haynes BF, Shaw GM, Hahn BH, Korber BT, Swanstrom R, Williamson C.** 2009. Quantitating the multiplicity of infection with human immunodeficiency virus

type 1 subtype C reveals a non-poisson distribution of transmitted variants. J Virol **83:**3556-3567.

16. **Chen J, Powell D, Hu WS.** 2006. High frequency of genetic recombination is a common feature of primate lentivirus replication. J Virol **80:**9651-9658.

17. **Chen J, Rhodes TD, Hu WS.** 2005. Comparison of the genetic recombination rates of human immunodeficiency virus type 1 in macrophages and T cells. J Virol **79:**9337-9340.

18. **Levy DN, Aldrovandi GM, Kutsch O, Shaw GM.** 2004. Dynamics of HIV-1 recombination in its natural target cells. Proceedings of the National Academy of Sciences of the United States of America **101:**4204-4209.

19. **Zhuang J, Jetzt AE, Sun G, Yu H, Klarmann G, Ron Y, Preston BD, Dougherty JP.** 2002. Human immunodeficiency virus type 1 recombination: rate, fidelity, and putative hot spots. J Virol **76:**11273-11282.

20. **Jetzt AE, Yu H, Klarmann GJ, Ron Y, Preston BD, Dougherty JP.** 2000. High rate of recombination throughout the human immunodeficiency virus type 1 genome. J Virol **74:**1234-1240.

21. **Chin MPS, Rhodes TD, Chen JB, Fu W, Hu WS.** 2005. Identification of a major restriction in HIV-1 intersubtype recombination. Proceedings of the National Academy of Sciences of the United States of America **102:**9002-9007.

22. **Iglesias-Sanchez MJ, Lopez-Galindez C.** 2002. Analysis, quantification, and evolutionary consequences of HIV-1 in vitro recombination. Virology **304:**392-402.

23. **Salazar-Gonzalez JF, Salazar MG, Keele BF, Learn GH, Giorgi EE, Li H, Decker JM, Wang S, Baalwa J, Kraus MH, Parrish NF, Shaw KS, Guffey MB, Bar KJ, Davis KL, Ochsenbauer-Jambor C, Kappes JC, Saag MS, Cohen MS, Mulenga J, Derdeyn CA, Allen S, Hunter E, Markowitz M, Hraber P, Perelson AS, Bhattacharya T, Haynes BF, Korber BT, Hahn BH, Shaw GM.** 2009. Genetic identity, biological phenotype, and evolutionary pathways of transmitted/founder viruses in acute and early HIV-1 infection. J Exp Med **206:**1273-1289.

24. **Schlub TE, Smyth RP, Grimm AJ, Mak J, Davenport MP.** 2010. Accurately measuring recombination between closely related HIV-1 genomes. PLoS Comput Biol **6:**e1000766.

25. **Pfeiffer JK, Topping RS, Shin NH, Telesnitsky A.** 1999. Altering the intracellular environment increases the frequency of tandem repeat deletion during Moloney murine leukemia virus reverse transcription. J Virol **73:**8441-8447.

26. **Operario DJ, Balakrishnan M, Bambara RA, Kim B.** 2006. Reduced dNTP interaction of human immunodeficiency virus type 1 reverse transcriptase promotes strand transfer. J Biol Chem **281:**32113-32121.

27. **Svarovskaia ES, Delviks KA, Hwang CK, Pathak VK.** 2000. Structural determinants of murine leukemia virus reverse transcriptase that affect the frequency of template switching. J Virol **74:**7171-7178.

28. **Galetto R, Moumen A, Giacomoni V, Veron M, Charneau P, Negroni M.** 2004. The structure of HIV-1 genomic RNA in the gp120 gene determines a recombination hot spot in vivo. J Biol Chem **279:**36625-36632.

29. **Shen W, Gao L, Balakrishnan M, Bambara RA.** 2009. A recombination hot spot in HIV-1 contains guanosine runs that can form a G-quartet structure and promote strand transfer in vitro. J Biol Chem **284:**33883-33893.

30. **Moumen A, Polomack L, Roques B, Buc H, Negroni M.** 2001. The HIV-1 repeated sequence R as a robust hot-spot for copy-choice recombination. Nucleic Acids Res **29:**3814-3821.

31. **Andersen ES, Jeeninga RE, Damgaard CK, Berkhout B, Kjems J.** 2003. Dimerization and template switching in the 5' untranslated region between various subtypes of human immunodeficiency virus type 1. J Virol **77:**3020-3030.

32. **Mikkelsen JG, Rasmussen SV, Pedersen FS.** 2004. Complementarity-directed RNA dimer-linkage promotes retroviral recombination in vivo. Nucleic Acids Res **32:**102-114.

33. **Dykes C, Balakrishnan M, Planelles V, Zhu Y, Bambara RA, Demeter LM.** 2004. Identification of a preferred region for recombination and mutation in HIV-1 gag. Virology **326:**262-279.

34. **Galetto R, Giacomoni V, Veron M, Negroni M.** 2006. Dissection of a circumscribed recombination hot spot in HIV-1 after a single infectious cycle. J Biol Chem **281:**2711-2720.

35. **Chin MP, Lee SK, Chen J, Nikolaitchik OA, Powell DA, Fivash MJ, Jr., Hu WS.** 2008. Long-range recombination gradient between HIV-1 subtypes B and C variants caused by sequence differences in the dimerization initiation signal region. Journal of molecular biology **377:**1324-1333.

36. **Gibbs JS, Regier DA, Desrosiers RC.** 1994. Construction and in vitro properties of HIV-1 mutants with deletions in "nonessential" genes. Aids Res. Hum. Retrovir. **10:**343-350.

37. **Smyth RP, Schlub TE, Grimm A, Venturi V, Chopra A, Mallal S, Davenport MP, Mak J.** 2010. Reducing chimera formation during PCR amplification to ensure accurate genotyping. Gene **469:**45-51.

38. **Meyer M, Stenzel U, Myles S, Prufer K, Hofreiter M.** 2007. Targeted high-throughput sequencing of tagged nucleic acid samples. Nucleic Acids Res **35:**e97.

39. **Goto N, Prins P, Nakao M, Bonnal R, Aerts J, Katayama T.** 2010. BioRuby: bioinformatics software for the Ruby programming language. Bioinformatics **26:**2617-2619.

40. **Margulies M, Egholm M, Altman WE, Attiya S, Bader JS, Bemben LA, Berka J, Braverman MS, Chen YJ, Chen Z, Dewell SB, Du L, Fierro JM, Gomes XV, Godwin BC, He W, Helgesen S, Ho CH, Irzyk GP, Jando SC, Alenquer ML, Jarvie TP, Jirage KB, Kim JB, Knight JR, Lanza JR, Leamon JH, Lefkowitz SM, Lei M, Li J, Lohman KL, Lu H, Makhijani VB, McDade KE, McKenna MP, Myers EW, Nickerson E, Nobile JR, Plant R, Puc BP, Ronan MT, Roth GT, Sarkis GJ, Simons JF, Simpson JW, Srinivasan M, Tartaro KR, Tomasz A, Vogt KA, Volkmer GA, Wang SH, Wang Y, Weiner MP, Yu P, Begley RF, Rothberg JM.** 2005. Genome sequencing in microfabricated high-density picolitre reactors. Nature **437:**376-380.

41. **Team RDC.** 2011. R: A Language and Environment for Statistical Computing. R Foundation for Statistical Computing, Vienna, Austria.

42. **Thompson JR, Marcelino LA, Polz MF.** 2002. Heteroduplexes in mixed-template amplifications: formation, consequence and elimination by 'reconditioning PCR'. Nucleic Acids Res **30:**2083-2088.

43. **Meyerhans A, Vartanian JP, Wain-Hobson S.** 1990. DNA recombination during PCR. Nucleic Acids Res **18:**1687-1691.

44. **Anderson RA, Eliason SL.** 1986. Recombination of homologous DNA fragments transfected into mammalian cells occurs predominantly by terminal pairing. Molecular and cellular biology **6:**3246-3252.

45. **Kuiken C, Foley B, Leitner T, Apetrei C, Hahn B, Mizrachi I, Mullins J, Rambaut A, Wolinsky S, Korber B.** 2010. HIV Sequence Compendium 2010. Theoretical Biology and Biophysics Group, Los Alamos National Laboratory, NM, LA-UR 10-03684.

46. **Di Giallonardo F, Zagordi O, Duport Y, Leemann C, Joos B, Kunzli-Gontarczyk M, Bruggmann R, Beerenwinkel N, Gunthard HF, Metzner KJ.** 2013. Next-Generation Sequencing of HIV-1 RNA Genomes: Determination of Error Rates and Minimizing Artificial Recombination. PLoS One **8:**e74249.

47. **Powell RLR, Lezeau L, Kinge T, Nyambi PN.** 2010. Longitudinal Quasispecies Analysis of Viral Variants in HIV Type 1 Dually Infected Individuals Highlights the Importance of Sequence Identity in Viral Recombination. Aids Res. Hum. Retrovir. **26:**253-264.

48. **Charpentier C, Nora T, Tenaillon O, Clavel F, Hance AJ.** 2006. Extensive recombination among human immunodeficiency virus type 1 quasispecies makes an important contribution to viral diversity in individual patients. J Virol **80:**2472-2482.

49. **Brown RJ, Peters PJ, Caron C, Gonzalez-Perez MP, Stones L, Ankghuambom C, Pondei K, McClure CP, Alemnji G, Taylor S, Sharp PM, Clapham PR, Ball JK.** 2011.

Intercompartmental recombination of HIV-1 contributes to env intrahost diversity and modulates viral tropism and sensitivity to entry inhibitors. J Virol **85:**6024-6037.

50. **Wain-Hobson S, Renoux-Elbe C, Vartanian JP, Meyerhans A.** 2003. Network analysis of human and simian immunodeficiency virus sequence sets reveals massive recombination resulting in shorter pathways. J Gen Virol **84:**885-895.

51. **Bretscher MT, Althaus CL, Muller V, Bonhoeffer S.** 2004. Recombination in HIV and the evolution of drug resistance: for better or for worse? Bioessays **26:**180-188.

52. **Vijay NN, Vasantika, Ajmani R, Perelson AS, Dixit NM.** 2008. Recombination increases human immunodeficiency virus fitness, but not necessarily diversity. J Gen Virol **89:**1467-1477.

53. **Kellam P, Larder BA.** 1995. Retroviral recombination can lead to linkage of reverse transcriptase mutations that confer increased zidovudine resistance. J Virol **69:**669-674.

54. **Mostowy R, Kouyos RD, Fouchet D, Bonhoeffer S.** 2011. The role of recombination for the coevolutionary dynamics of HIV and the immune response. PLoS One **6:**e16052.

55. **Streeck H, Li B, Poon AF, Schneidewind A, Gladden AD, Power KA, Daskalakis D, Bazner S, Zuniga R, Brander C, Rosenberg ES, Frost SD, Altfeld M, Allen TM.** 2008. Immune-driven recombination and loss of control after HIV superinfection. J Exp Med **205:**1789-1796.

56. **Liu SL, Mittler JE, Nickle DC, Mulvania TM, Shriner D, Rodrigo AG, Kosloff B, He X, Corey L, Mullins JI.** 2002. Selection for human immunodeficiency virus type 1 recombinants in a patient with rapid progression to AIDS. J Virol **76:**10674-10684.

57. **Nishimura Y, Shingai M, Lee WR, Sadjadpour R, Donau OK, Willey R, Brenchley JM, Iyengar R, Buckler-White A, Igarashi T, Martin MA.** 2011. Recombination-mediated changes in coreceptor usage confer an augmented pathogenic phenotype in a nonhuman primate model of HIV-1-induced AIDS. J Virol **85:**10617-10626.

58. **Shi B, Kitchen C, Weiser B, Mayers D, Foley B, Kemal K, Anastos K, Suchard M, Parker M, Brunner C, Burger H.** 2010. Evolution and recombination of genes encoding HIV-1 drug resistance and tropism during antiretroviral therapy. Virology **404:**5-20.

59. **Wooley DP, Bircher LA, Smith RA.** 1998. Retroviral recombination is nonrandom and sequence dependent. Virology **243:**229-234.

60. **Johnson VA, Calvez V, Gunthard HF, Paredes R, Pillay D, Shafer R, Wensing AM, Richman DD.** 2011. 2011 update of the drug resistance mutations in HIV-1. Top Antivir Med **19:**156-164.

61. **Simon-Loriere E, Martin DP, Weeks KM, Negroni M.** 2010. RNA structures facilitate recombination-mediated gene swapping in HIV-1. J Virol **84:**12675-12682.

62. **Galli A, Kearney M, Nikolaitchik OA, Yu S, Chin MP, Maldarelli F, Coffin JM, Pathak VK, Hu WS.** 2010. Patterns of Human Immunodeficiency Virus type 1 recombination ex vivo provide evidence for coadaptation of distant sites, resulting in purifying selection for intersubtype recombinants during replication. J Virol **84:**7651-7661.

63. **Watts JM, Dang KK, Gorelick RJ, Leonard CW, Bess JW, Jr., Swanstrom R, Burch CL, Weeks KM.** 2009. Architecture and secondary structure of an entire HIV-1 RNA genome. Nature **460:**711-716.

64. **Klarmann GJ, Schauber CA, Preston BD.** 1993. Template-directed pausing of DNA synthesis by HIV-1 reverse transcriptase during polymerization of HIV-1 sequences in vitro. J Biol Chem **268:**9793-9802.

65. **Roda RH, Balakrishnan M, Kim JK, Roques BP, Fay PJ, Bambara RA.** 2002. Strand transfer occurs in retroviruses by a pause-initiated two-step mechanism. J Biol Chem **277:**46900-46911.

66. **Gao L, Balakrishnan M, Roques BP, Bambara RA.** 2007. Insights into the multiple roles of pausing in HIV-1 reverse transcriptase-promoted strand transfers. J Biol Chem **282:**6222-6231.

67. **Hanson MN, Balakrishnan M, Roques BP, Bambara RA.** 2005. Effects of donor and acceptor RNA structures on the mechanism of strand transfer by HIV-1 reverse transcriptase. Journal of molecular biology **353:**772-787.

68. **Josefsson L, Palmer S, Faria NR, Lemey P, Casazza J, Ambrozak D, Kearney M, Shao W, Kottilil S, Sneller M, Mellors J, Coffin JM, Maldarelli F.** 2013. Single cell analysis of lymph node tissue from HIV-1 infected patients reveals that the majority of CD4+ T-cells contain one HIV-1 DNA molecule. PLoS Pathog **9:**e1003432.

69. **Jung A, Maier R, Vartanian JP, Bocharov G, Jung V, Fischer U, Meese E, Wain-Hobson S, Meyerhans A.** 2002. Recombination: Multiply infected spleen cells in HIV patients. Nature **418:**144.

70. **Josefsson L, King MS, Makitalo B, Brannstrom J, Shao W, Maldarelli F, Kearney MF, Hu WS, Chen J, Gaines H, Mellors JW, Albert J, Coffin JM, Palmer SE.** 2011. Majority of CD4+ T cells from peripheral blood of HIV-1-infected individuals contain only one HIV DNA molecule. Proceedings of the National Academy of Sciences of the United States of America **108:**11199-11204.

Figures

Figure 1: Recombination rate variation in gag and pol. Recombination rates were measured in 39 genome regions ranging from 21nt to 159nt in length (denoted by horizontal bars) in *gag* and *pol*. The average number of recombination events per nucleotide per round of infection (REPN) are shown on the y-axis with nucleotide position relative to the beginning of the NL43 5' LTR shown on the x-axis.

Figure 2: Recombination rate hotspots are consistent between viral phenotypes and PBMC blood donors. (A,C) Recombination rates are compared between two viral phenotypes R5 and X4 and between 5 blood donors with the average number of recombination events per nucleotide per round of infection (REPN) shown on the y-axis and nucleotide position relative to the beginning of the NL43 5' LTR shown on the x-axis (B) Correlation between the recombination rates of two viruses differing in viral phenotype, with REPN shown on both axes.

Figure 3: Recombination hotspots are not a product of marker design. To check if recombination rate hotspots are driven by the choice of silent codon modifications we measured the recombination rate in two different marker configurations, MK_{high} and MK_{low} for (A) CCR5(R5)-tropic viruses (C) CXCR4(X4)-tropic virus, and performed viral replicates of identical virues (E). (A, C, D) Recombination rates with the average number of recombination events per nucleotide per round of infection (REPN) shown on the y-axis and nucleotide position relative to the beginning of the NL43 5' LTR shown on the x-axis. (B, D) Correlations between the recombination rates of MK_{high} and MK_{low} viruses with REPN shown on both axes. (F) Correlation between the recombination rates of MK_{high} replicate infections with REPN shown on both axes. Correlations are Pearson product moment correlations.

Figure 4: Schematic of marker configurations, and how to compare between them. (A) In this study, recombination is measured between wildtype virus and a marker system with silent codon modifications 'markers' that do not affect any viral proteins or packaging (marker configuration

MK$_{high}$). To test that these codon modifications do not influence our recombination rate measurements, a second marker system virus is created where the codon modifications occur at different nucleotide positions (marker configuration MK$_{low}$). (B) To compare between marker configurations, MK$_{high}$ is used to predict what would be measured as the recombination rate, if MK$_{low}$ was used. This prediction can them be directly compared to the experimental results for MK$_{low}$. For each interval in MK$_{low}$ the MK$_{high}$ prediction is calculated by averaging the overlapping MK$_{high}$ interval's recombination rate, and weighting this average by the proportion of overlap.

Figure 5: 95% confidence intervals for the recombination rate in each region for the R5 phenotype. We fit a generalized linear model to the dataset to calculate the statistical significance of recombination hot and cold spots, after accounting for confounding factors such as viral phenotype and donor. The model estimates the standard error in recombination rate for each genome region, from which a 95% confidence interval is obtained. Those intervals that do not overlap the average rate are bolded. (A) Recombination rate per nucleotide for each genome segment in R5 averaged over all donors. Horizontal bars represent the length of the genome region. 95% confidence intervals are Bonferroni corrected for the multiple comparisons. (B) Statistically significant hot and cold spots corresponding to genome location.

R5 virus	Donor 2	Donor 3	Donor 4	Donor 5
Donor 1	r = 0.58, p = 0.003	r = 0.71, p < 0.001	r = 0.58, p < 0.001	r = 0.66, p < 0.001
Donor 2		r = 0.44, p = 0.04	r = 0.58, p = 0.003	r = 0.64, p < 0.001
Donor 3			r = 0.54, p = 0.001	r = 0.61, p < 0.001
Donor 4				r = 0.63, p < 0.001

Table 1: Between patient correlations for R5. To investigate whether recombination hot and cold spot locations are similar across different donors, the recombination rate for each interval and donor was calculated (Figure 2C). The pair-wise correlations on the interval specific recombination

rate across donors were all positive and significant, indicating that recombination hot and cold spot locations are consistent across donors.

Model number	Description	Residual deviance	DF (# of parameters)	p-value (when compared to model)
1	One average recombination rate	1883	274 (1)	
2	Rate depends on virus	1813	273 (2)	<0.001 (1)
3	Rate depends on donor	1470	270 (5)	<0.001 (1)
4	Rate depends on virus and donor	1424	269 (6)	<0.001 (1, 2 or 3)
5	Rate depends on virus, donor and interval	696	231 (44)	<0.001 (4)

Table 2: Generalized linear models (GLMS) fitted. GLMs are a good analytic framework for investigating the effects of nucleotide position on recombination rate after accounting for the confounding effects of virus phenotype and blood donor. To build up the appropriate complexity for this analysis, a base model (model 1) with one average recombination rate fitted to all of the data pooled together was created. We next fitted more complex models with a recombination rate for each virus (model 2), a recombination rate for each donor (model 3) and a recombination rate that depends on both donor and phenotype (model 4). These models increase the number the complexity of the analysis which is reflected in the increase in number of parameters and decrease in the degrees of freedom (DF column). However, this increased complexity is statistically justified, as the reduction in deviance (a measure of error in the model) is sufficiently large. This indicates that viral phenotype and donor are confounding effects and should be included in the final model. In the final model recombination rates depend on phenotype, donor and genome interval (model 5). This model's increase in complexity is also justified by the reduction in deviance. The final model shows that genome position is an independent predictor for recombination rate, that the hot and cold spots we observe in our data are statistically significant, and that the location of recombination hot and cold spots are consistent across viral phenotypes and donors.

Interval	RR difference to mean (x10^{-3})	P-value	Nucleotide Position start (from 5' LTR)	Nucleotide Position end (from 5' LTR)	Interval length	Amino Acid 5' interval	Amino Acid 3' interval
G_H2	0.38	<0.001	912	984	72	E42	Q65
G_H3	-0.09		984	1032	48	P66	T81
G_H4	-0.10		1032	1113	81	I82	Q108
G_H5	0.51	<0.001	1113	1266	153	N109	V159
G_H6	-0.74	<0.001	1266	1287	21	E160	P166
G_H7	0.49	<0.001	1287	1374	87	E167	Q195
G_H8	0.55	<0.001	1374	1476	102	A196	R229
G_H9	-0.31		1476	1524	48	E230	E245
G_H10	-0.56	<0.001	1524	1560	36	Q246	P257
G_H11	0.32	<0.05	1560	1719	159	V258	S310
G_H12	0.95	<0.001	1719	1821	102	Q311	E344
G_H13	1.11	<0.001	1821	1896	75	E345	Q369
G_H14	-0.31	<0.05	1896	1947	51	V370	Q386
P_H6	0.78	<0.05	2573	2615	42	V8	K22
P_H7	-0.22		2615	2651	36	Q22	L34
P_H8	-0.55		2651	2681	30	V34	E44
P_H9	0.55		2681	2726	45	G44	P59
P_H10	-0.17		2726	2771	45	V59	L74
P_H11	0.11		2771	2825	54	V74	L92
P_H12	-0.63	<0.001	2825	2870	45	G92	T107

P_H13	0.45		2870	2909	39	V107	L120
P_H14	-0.02		2909	2966	57	D120	T139
P_H15	-0.54	<0.05	2966	3011	45	P139	K154
P_H16	-0.46		3011	3065	54	G154	R172
P_H17	0.32		3065	3116	51	K172	V189
P_H18	-0.10		3116	3167	51	G189	R206
P_H19	0.57	<0.01	3167	3218	51	Q206	K223
P_H20	0.43	<0.05	3218	3290	72	E223	P247
P_H21	-0.93	<0.001	3290	3326	36	E247	K259
P_H22	-0.46	<0.001	3326	3383	57	L259	Q278
P_H24	-0.49	<0.01	3425	3479	54	V292	L310
P_H26	-0.13		3530	3599	69	A327	K350
P_H27	0.11		3599	3650	51	T350	Q367
P_H28	0.68	<0.01	3650	3680	30	L367	T377
P_H29	0.41	<0.05	3680	3746	66	E377	E399
P_H30	0.46		3746	3815	69	A399	L422
P_H31	-0.72	<0.01	3815	3860	45	V422	A437
P_H32	-0.35		3860	3905	45	E437	L452
P_H33	-1.29	<0.001	3905	3930	25	G453	D460

Table 3: Locations of hotspots and coldspots. Using the final GLM (Table 2, model 5) we predicted the recombination rate for each interval after adjusting for the effects of viral phenotype and donor variability (Figure 5). From the estimate of standard error for each interval, we determined which regions are significantly different to the average recombination rate across *gag* and *pol*. Intervals without p-values were not significant at the 0.05 level.

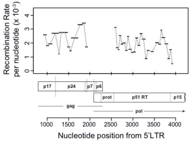
Recombination Rate
per nucleotide (x 10⁻³)
0
1
2
3
4
p17
p24
p7
p6
prot
p51 RT
p15
gag
pol
1000
1500
2000
2500
3000
3500
4000
Nucleotide position from 5'LTR

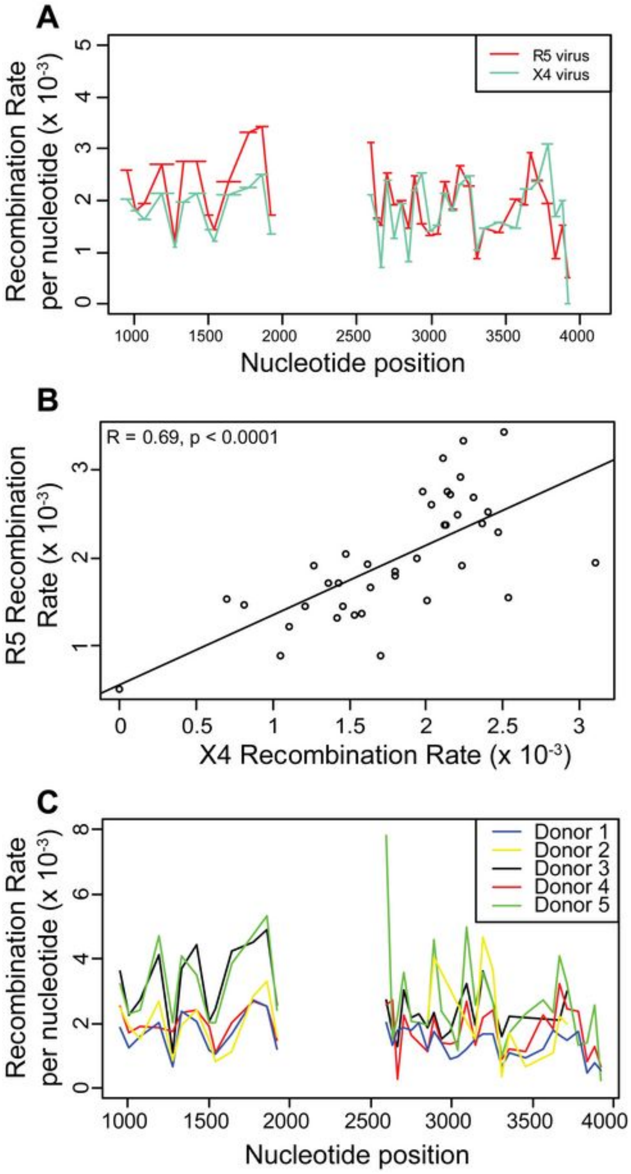
A
Recombination Rate per nucleotide (x 10^{-3})
0
1
2
3
4
5
1000
1500
2000
2500
3000
3500
4000
Nucleotide position
R5 virus
X4 virus
B
R = 0.69, p < 0.0001
R5 Recombination Rate (x 10^{-3})
1
2
3
0
0.5
1
1.5
2
2.5
3
X4 Recombination Rate (x 10^{-3})
C
Recombination Rate per nucleotide (x 10^{-3})
0
2
4
6
8
1000
1500
2000
2500
3000
3500
4000
Nucleotide position
Donor 1
Donor 2
Donor 3
Donor 4
Donor 5

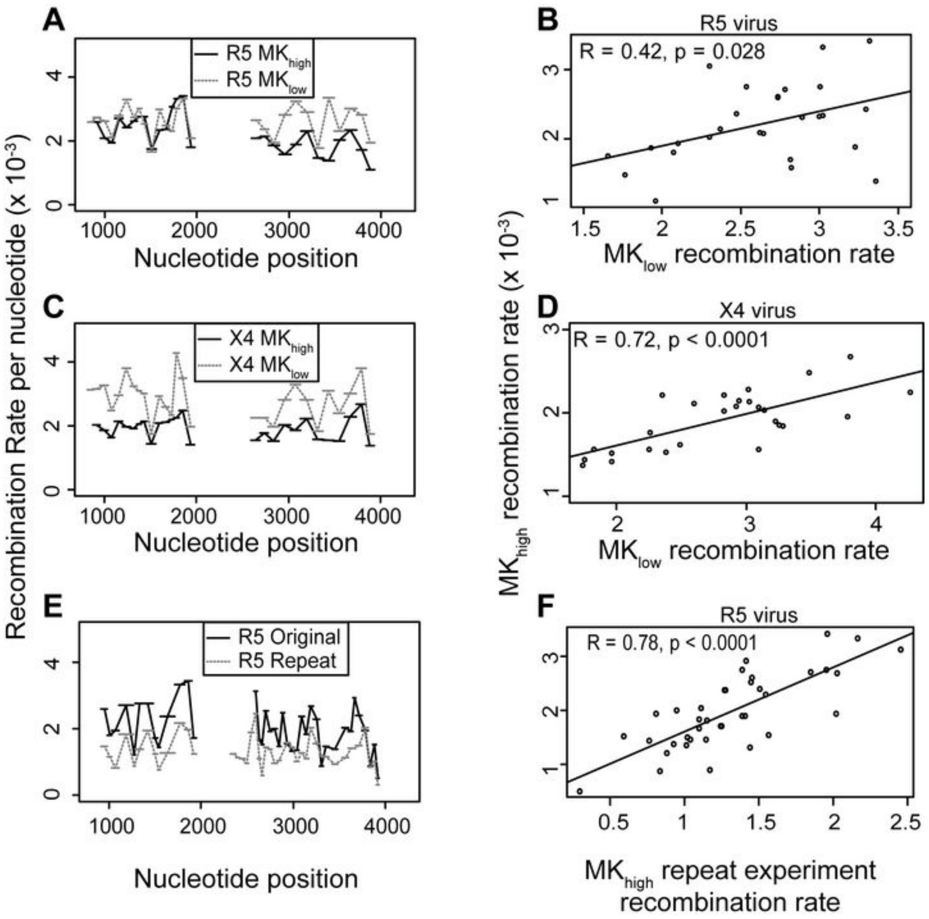
A
R5 MK$_{high}$
R5 MK$_{low}$
0
2
4
1000
2000
3000
4000
Nucleotide position
B
R5 virus
R = 0.42, p = 0.028
1
2
3
1.5
2
2.5
3
3.5
MK$_{low}$ recombination rate
C
X4 MK$_{high}$
X4 MK$_{low}$
0
2
4
1000
2000
3000
4000
Nucleotide position
D
X4 virus
R = 0.72, p < 0.0001
1
2
3
2
3
4
MK$_{low}$ recombination rate
MK$_{high}$ recombination rate (x 10^{-3})
Recombination Rate per nucleotide (x 10^{-3})
E
R5 Original
R5 Repeat
0
2
4
1000
2000
3000
4000
Nucleotide position
F
R5 virus
R = 0.78, p < 0.0001
1
2
3
0.5
1
1.5
2
2.5
MK$_{high}$ repeat experiment
recombination rate

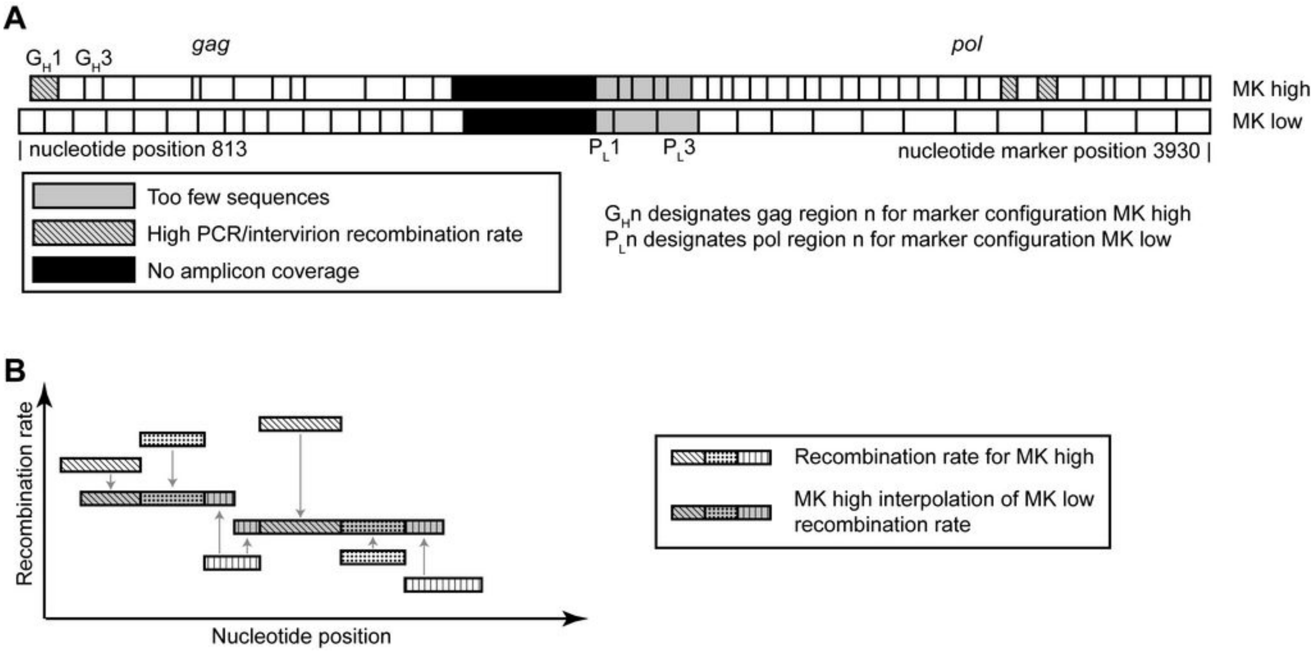
A
gag
pol
G_H1
G_H3
MK high
MK low
| nucleotide position 813
P_L1
P_L3
nucleotide marker position 3930 |
Too few sequences
High PCR/intervirion recombination rate
No amplicon coverage
G_Hn designates gag region n for marker configuration MK high
P_Ln designates pol region n for marker configuration MK low
B
Recombination rate
Nucleotide position
Recombination rate for MK high
MK high interpolation of MK low recombination rate

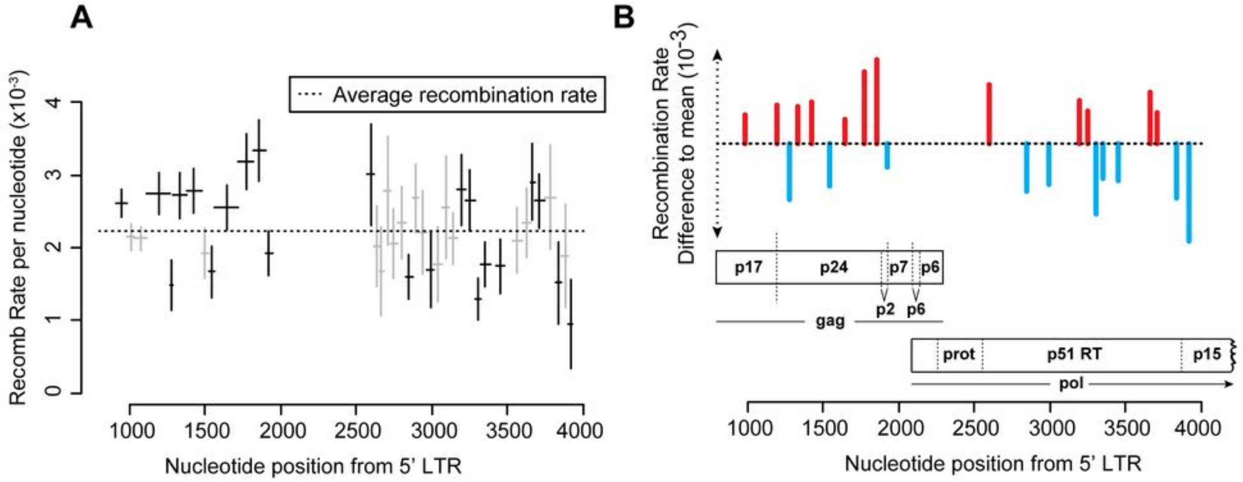
A
Average recombination rate
Recomb Rate per nucleotide (x10^{-3})
0
1
2
3
4
1000
1500
2000
2500
3000
3500
4000
Nucleotide position from 5' LTR
B
Recombination Rate
Difference to mean (10^{-3})
p17
p24
p7
p6
p2
p6
gag
prot
p51 RT
p15
pol
1000
1500
2000
2500
3000
3500
4000
Nucleotide position from 5' LTR